Journal of Medicinal Chemistry

Article

Antimalarial Pyrido[1,2-a]benzimidazoles: Lead Optimization, Parasite Life Cycle Stage Profile, Mechanistic Evaluation, Killing Kinetics and In Vivo Oral Efficacy in a Mouse Model

Kawaljit Singh, John Okombo, Christel Brunschwig, Ferdinand Ndubi, Linley Barnard, Chad Wilkinson, Peter M. Njogu, Mathew Njoroge, Lizahn Laing, Marta Machado, Miguel Prudêncio, Janette Reader, Mariette E. Botha, Sindisiwe H. Nondaba, Lyn-Marie Birkholtz, Sonja Lauterbach, Alisje Churchyard, Theresa L. Coetzer, Jeremy N. Burrows, Clive Leonard Yeates, Paolo Denti, Lubbe Wiesner, Timothy J Egan, Sergio Wittlin, and Kelly Chibale

J. Med. Chem., **Just Accepted Manuscript** • DOI: 10.1021/acs.jmedchem.6b01641 • Publication Date (Web): 17 Jan 2017

Antimalarial Pyrido[1,2-*a*]benzimidazoles: Lead Optimization, Parasite Life Cycle Stage Profile, Mechanistic Evaluation, Killing Kinetics and In Vivo Oral Efficacy in a Mouse Model

Kawaljit Singh[†,#], John Okombo[†], Christel Brunschwig[∞], Ferdinand Ndubi[†], Linley Barnard[†], Chad Wilkinson[†], Peter M. Njogu[¥], Mathew Njoroge[∞],Lizahn Laing[∞], Marta Machado[Ψ], Miguel Prudêncio[Ψ], Janette Reader[‡], Mariette Botha[‡], Sindisiwe Nondaba[‡], Lyn-Marie Birkholtz[‡], Sonja Lauterbach[§], Alisje Churchyard[§], Theresa L. Coetzer[§],Jeremy N. Burrows[P], Clive Yeates[ζ], Paolo Denti[∞], Lubbe Wiesner[∞], Timothy J. Egan[†], Sergio Wittlin[◊,∫], and Kelly Chibale[,†,#]*

[†]Department of Chemistry, University of Cape Town, Rondebosch 7701, South Africa; [#] South African Medical Research Council, Drug Discovery and Development Research Unit, Department of Chemistry and Institute of Infectious Disease and Molecular Medicine, University of Cape Town, Rondebosch 7701, South Africa; [¥]Department of Pharmaceutical Chemistry, University of Nairobi, P.O. Box 19676, Nairobi, 00202, Kenya; [∞]Division of Clinical Pharmacology, Department of Medicine, University of Cape Town, Observatory, 7925, South Africa; [Ψ] Instituto de Medicina Molecular, Faculdade de Medicina, Universidade de Lisboa, Av. Prof. Egas Moniz, 1649-028 Lisboa, Portugal; [‡]Department of Biochemistry, Institute for

Sustainable Malaria Control, University of Pretoria, Private bag X20, Hatfield 0028, South Africa;[§]Wits Research Institute for Malaria, Faculty of Health Sciences, University of the Witwatersrand and National Health Laboratory Service, Johannesburg 2193, South Africa; [Þ]Medicines for Malaria Venture, ICC, Route de Pré-Bois 20, P.O. Box 1826, 1215 Geneva, Switzerland; [ζ]Inpharma Consultancy, 6 Dudley Hill Close, Welwyn, Herts AL60QQ, UK; [◊]Swiss Tropical and Public Health Institute, Socinstrasse 57, 4002 Basel, Switzerland; [ʃ]University of Basel, 4003 Basel, Switzerland

ABSTRACT: Further structure activity relationship (SAR) studies on the recently identified pyrido[1,2-*a*]benzimidazole (PBI) antimalarials, have led to the identification of potent, metabolically stable compounds with improved in vivo oral efficacy in the *P. berghei* mouse model and additional activity against parasite liver and gametocyte stages, making them potential candidates for preclinical development. Inhibition of haemozoin formation possibly contributes to the mechanism of action.

INTRODUCTION

Malaria,a parasitic disease caused by parasites of the *Plasmodium* genus,remains a global public health concern due to its morbidity and mortality, with approximately 214 million new clinical cases and about 438,000 deaths reported in 2015.[1]Mammalian infection is initiated by the bite of *Plasmodium*-infected female *Anopheles* mosquitoes. An asymptomatic but obligatory developmental phase in the liver ensues, leading to the release of newly formed parasites into the bloodstream, where they infect red blood cells and cause disease symptoms.[2] Transmission of the parasite to the mosquito vector occurs when the latter ingests circulating gametocytes, initiating the sexual stage of the parasite's lifecycle. Chemotherapy represents one of the most effective control measures to mitigate the malaria burden, with the World Health Organization (WHO) presently recommending the use of artemisinin combination therapies (ACT) for treatment of uncomplicated malaria. However, there is compelling evidence from Southeast Asia describing the emergence and spread of ACT tolerance, which is characterised by reduced clearance rates of *Plasmodium falciparum* parasites.[3, 4] This underscores the urgent need to expand the antimalarial

drug arsenal by exploring and developing new compound classes, preferably with a combination of novel modes of action, multi-stage activity, good safety profile and efficacy at low doses.

The benzimidazole motif is a recognized privileged scaffold in medicinal chemistry due to its capacity to interact with numerous biological systems,[5] leading to a wide variety of biological activities, including antimalarial activity.[6-9] Pyrido[1,2-*a*]benzimidazoles (PBIs), previously investigated for antibacterial, antifungal, antiviral and antitumor activities,[10] were recently shown to be a novel antimalarial chemotype.[11] The lead compound from the previous studies **8** (Figure 1), showed high antiplasmodial activity in vitro (IC_{50} (*Pf*NF54) = 0.11μM; IC_{50} (*Pf*K1) = 0.12μM) and promising oral efficacy (95% at 4×50 mg/kg p.o) in vivo in the rodent *P. berghei* model. However, pharmacokinetic (PK) studies indicated saturation in oral absorption at low doses, presumably due to poor dissolution or solubility, which may be a factor in limiting oral efficacy. Herein, we describe further structure activity relationship (SAR) investigations (SAR_1-$_4$) around the scaffold of compound **8** (Figure 2), partly to explore the potential for generating derivatives with an improved PK profile but also to explore the effect on activity of changes around parts of the scaffold not previously investigated, with the goal of improving oral activity in the mouse model to confirm if this series has potential for further development.

The SAR studies can be broken down according to Fig. 2:

- SAR_1- replacement of the alkylamino side chain with various alkyl, cycloalkyl and heterocyclic moieties containing water-solubilizing H-bonding groups, encompassing hydroxypyrrolidine, azetidinol, hydroxypiperidine, piperazine or sulfonamide substituents.

- SAR_2- introduction of small hydrophobic substituents at the C-2 position to favor non co-planar conformations of the C-3 aryl, lowering the crystal packing energies and consequently improving aqueous solubility.[12]
- SAR_3- replacement of the 4-trifluoromethylphenyl (4-CF_3Ph) at the C-3 position with substituted or unsubstituted phenyl rings and with saturated systems or cycloalkyl groups and introduction of water-solubilizing H-bonding groups including ester, sulfinyl, sulfone and sulfoxide substituents on the C-3 phenyl ring.
- SAR_4- introduction of substituents on the previously[11] unexplored left aromatic ring, including replacement with the less lipophilic pyridyl ring.

The in vitro antiplasmodial activities of synthesized derivatives against chloroquine-sensitive (CQ-S) and multidrug resistant *P. falciparum* strains as well as in vivo efficacy in *P. berghei*-infected mice are reported. Additionally, we present metabolic stability, killing kinetics, gametocytocidal and liver stage activity data on a subset of the compounds. Some mechanistic studies were done, focusing on the potential for inhibition of haemozoin (Hz) formation, on the hypothesis that the ability of PBIs to adopt flat conformations would allow for π-π stacking interactions with ferriprotoporphyrin IX (Fe(III)PPIX), a toxic by-product of host haemoglobin degradation, thus leading to inhibition of Hz crystal formation and consequent parasite death.

Chemistry: The synthesis of target PBI derivatives was relatively straightforward using published procedures (Scheme 1).[11]

Biology: In vitro antiplasmodial activity and cytotoxicity: All compounds were evaluated for in vitro antiplasmodial activity against the CQS *Pf*NF54 strain; those with submicromolar activity (34/62 compounds) were further tested against the multidrug resistant *Pf*K1 strain and for mammalian cytotoxicity against Chinese hamster ovary (CHO) cell lines. The results are summarized in **Tables 1-3**. In general, activity of the compounds ranged from 0.02-0.95 μM and 0.02-1.07 μM against *Pf*NF54 and *Pf*K1, respectively, with 28/34 exhibiting submicromolar potency against both strains.

With regard to SAR:

1. SAR_1 – variation in the aminoalkyl side chain, with a heterocyclic, cyclic and alkyl substituents containing H-bonding groups (**9**–**38**; **Table 1**).
    - The only improvement in vitro was found in replacement of the N-ethyl in **8** with a 3-hydroxy pyrrolidine (**11**), showing ~ 3x reduction in IC_{50} relative to **8**, with better selectivity.
    - Introduction of the same side chain present in chloroquine (**16**, **17**) resulted in a significant drop in activity and poor selectivity.

2. SAR_2 – Introduction of -Me or –F substituents at C-2 (**66** – **69**; **Table 3**).
    - Retaining the N-ethyl ethylenediamine side chain of **8** and introducing a C-2 Me (**66**) or F (**67**) resulted in a significant loss in activity, with a 10-50x increase in *Pf*NF54 IC_{50}.
    - Activity of the 2-Me and 2-F derivatives was improved by introduction of the 3-hydroxypyrrolidinyl side chain (**68**, **69**), consistent with the previous observations from

SAR_1 (see **11**; **Table 1**), with the 2-F analogue (**69**) now showing comparable activity to **8** with significantly better selectivity.

3. SAR_3 – Replacement of the 4-CF_3Ph in **8** with unsubstituted as well as substituted phenyl rings and cycloalkyl groups (**39**–**53**; **Table 2**).
    - Varying the position of the -CF_3 group from the para (**8**) to the meta-position (**40**) had only a slight effect on activity. The unsubstituted phenyl and a range of ortho (**43**), meta (**44**), para (**41**, **42**, **46**, **50**) and di-substituted derivatives (**45**) all retained significant activity (*Pf*NF54 IC_{50} <1 μM), with only **50** showing a significant improvement in selectivity.
    - Substitution with a para –COOMe (**47**), -SMe (**48**), or -SOMe (**49**) significantly lowered activity, as did replacing the 4-CF_3Ph with a -CF_3 (**51**).
    - Cycloalkyl groups at C-3, including cyclohexyl (**52**) and cyclopentyl (**53**), were well tolerated but showed no improvement in selectivity.

.

4. SAR_4– Substitution on the benzimidazole (**54**–**65**; **Table 3**)
    - Substitution at C-7, C-8 or C-9 with Cl or Br, including multiple substitutions, was well tolerated, providing in some cases a significant improvement in activity (**54**, **56**, **59**, and **60**) and selectivity (**54**, **59**, and **60**).
    - Replacing the phenyl with a pyridyl (**64**, **65**) had either no effect or lowered antiplasmodial activity, depending on the position of the ring nitrogen, and was accompanied by poor selectivity.

- Replacing the N-ethyl ethylenediamine side chain in some of the more active compounds (**59**, **60**) with various cycloalkylamino side chains did not give any improvement in activity and generally lowered selectivity (**61**–**63**), consistent with the previous observations in SAR_1.

Physicochemical properties (**Table 4**)**:** From the range of analogues evaluated the following observations can be made:

- Permeability generally ranged from moderate to high at pH 6.5, indicative that permeability is unlikely to be a limiting factor in the oral absorption of these compounds from the gastrointestinal tract.
- Some improvement in solubility was achieved through introduction of a 2-F (**67**, **69**), although the corresponding 2-Me derivatives (**66**, **68**) were poorly soluble, despite the anticipation that distortion in the planarity of resulting from C-2 substitution would reduce the crystal packing energy thus helping dissolution in water.
- Introduction of water solubilizing groups like sulfone (**50**) did improve solubility but this proved detrimental to permeability.
- Replacement of the 4-CF_3Ph with a saturated ring (**52**) resulted in a slight improvement in solubility but at the expense of reduced microsomal stability.
- Predicted lipophilicity was relatively high (logP >3 for most compounds). For SAR_1 and SAR_3 analogues, increased lipophilicity was associated with better permeability while lower lipophilicity to better solubility, except for **17** with high logP but good solubility. There was no apparent relationship between lipophilicity and metabolic

stability for this series of compounds, suggesting that structural changes had a greater contribution to these properties than lipophilicity.

Metabolic stability in liver microsomes (**Table 4**)**:** The most active compounds in the in vitro antiplasmodial assay were assessed for metabolic stability in mouse and human liver microsomes (MLMs and HLMs, respectively). Most compounds showed no significant interspecies difference in microsomal stability and the following trends were observed:

- Introduction of a piperidinyl (**20**, **26**) or CQ-like side chain **(17)** led to a significant decrease in microsomal stability, with the exception of **36,** where the piperidinyl ring was directly linked to the PBI scaffold.
- 2-Methyl substitution (SAR_2) was not detrimental to microsomal stability **(66)**, but surprisingly the 2-F analogue (**67**) was significantly less stable.
- Variation in the substitution on the C-3 aryl (SAR_3) had a significant effect on stability, with the dichloro derivative (**45**) showing significantly poorer stability compared to **8**.
- The more active compounds with halogen substitution on the benzimidazole (SAR_4; **54**, **57**, **59**, **60**) did not show any significant difference in microsomal stability relative to **8**.

In vivo efficacy in the mouse *P. berghei* model (Table 5): Compounds with good antiplasmodial activity, reasonable solubility and high microsomal stability were assessed for in vivo efficacy in *P. berghei*-infected mice, dosing orally at 4 x 50 mg/kg; if mice were cured lower doses were evaluated (4 x 30 mg/kg, 4 x 10 mg/kg and 4 x 3 mg/kg). Parasitemia reduction in *P. berghei* in vivo efficacy testing helped to efficiently prioritize compounds in the knowledge

that those with good efficacy must have exposure. PK was followed up in detail on those that were most interesting. In summary:

- Compound **44**, less active than **8** in vitro but with slightly superior microsomal stability, showed slightly better in vivo efficacy compared to **8**, with a single cure at 4 x 50 mg/kg.
- Compound **57**, with comparable in vitro activity and microsomal stability to **8**, was not curative at 4 x 50 mg/kg.
- Compounds **59** and **60**, with significantly better in vitro activity and comparable microsomal stability to **8**, were completely curative at 4 x 50 mg/kg; **59** proving better at 4 x 30 mg/kg. At lower doses (4 x 10 mg/kg and 4 x 3 mg/kg), the mice were not cured (MSD of 16 – 18) although parasitemia was still reduced by > 99%.

Pharmacokinetic studies (Table 6). Studies were performed in mice dosed orally (p.o) at 10 mg/kg and intravenously (i.v.) at 2.5 mg/kg with compounds **59** and **60**. Since the elimination phase was not captured in the standard 24 h sampling period and non-compartmental analysis could not provide reliable parameter estimates, the data were interpreted with nonlinear mixed-effects modeling where a two-compartment disposition model was used, with first-order absorption and elimination. Both IV and oral data were fit in the same model, and bioavailability fixed to 100% for the IV infusion and estimated for the oral formulation. Between-mouse variability was included in the absorption rate constant, plasma clearance, and oral bioavailability. The PK parameters from the model were used to derive the exposure metrics in **Table 6**.

Both **59** and **60** were slowly absorbed when dosed orally (T_{max} of ≥10 h) and were slowly eliminated (i.e. CL<30 mL/min/kg). Considered in relation to the previous PK studies on **8**,[11] which showed broadly similar pharmacokinetics to **59** and **60**, it would appear that the significant improvement in efficacy of **59** and **60** in *P. berghei*-infected mice is likely to be due more to their better inherent antimalarial activity than improved pharmacokinetics.

Gametocytocidal and liver stage activity (Table 7). The potential of this compound class to act as dual or triple-action antimalarials was determined by evaluating their gametocytocidal potency[13] and liver stage activity. Compound **8** and a range of 17 new analogues were tested against early (EG; >90% stage II/III) and late (LG; >95% stage IV/V) gametocytes. The potential for inhibition of liver stage *Plasmodium* infection was assessed using a model with a *P. berghei* infected human hepatoma cell line (HuH 7).[14] Compounds **54** and **59,** with good in vitro blood stage activity, also showed comparable activity against both EG and LG, whilst others (**8**, **42**, **52**) showed a degree of stage-specific potency for LG gametocytes, indicated by a >2-fold change in IC_{50}.

Initial screening at 1 μM, 5 μM and 10 μM on liver stage infection and cell confluence using luciferase-expressing parasites and a luminescence-based method[15] established the non-toxicity of the test compounds, with no significant effect on cell proliferation. Compounds **26**, **66** and **69** led to the strongest decrease in infection at the lowest concentration tested (1 μM) and a subsequent dose-response analysis confirmed their activity. Compound **69**, which also had good blood stage activity (*Pf*K1 IC_{50}: 0.17 μM), was the most potent inhibitor in the *P. berghei* liver stage assay (IC_{50}: 1.42 μM), significantly more active than primaquine (PMQ) (IC_{50}: 8.42 μM), albeit less active than atovaquone (IC_{50}: 1.1 nM).[16] It should be noted that PMQ's activity in vivo is dependent on its oxidation to active metabolites[17] and, as such, the compound's IC_{50} in vitro

does not necessarily represent its in vivo potency. Compounds **26** (IC_{50}: 3.31 μM) and **66** (IC_{50}: 2.85 μM) also showed a degree of activity in the in vitro liver stage assay, in addition to their blood stage activity.

Speed of action and mechanistic evaluation. There was a suspicion from the previous studies on **8** in the *P. berghei* mouse model that the compounds might be inherently slow acting. To investigate this further a cross section of 9 compounds were run through a [^{3}H] hypoxanthine incorporation assay designed to assess their killing speed between at 24, 48, and 72 h.[18] The IC_{50} values of pyrimethamine, **11** and **69** were respectively 6-, 18- and 22- fold higher at 24 h compared to 72 h (**Figure 4**), indicating that these compounds were slow acting; it may be noteworthy that **11** and **69** have the 3-hydoxypyrrolidinyl side chain. However, **8**, **20**, **17** and **44** appeared to be faster acting (IC_{50} (24 h)/IC_{50} (72 h) < 1.5), comparable to CQ and AS, while **9**, **54** and **59** could be classified as neither fast or slow, with (IC_{50} (24 h)/ IC_{50} (72 h) 1.5 - 2). Overall, albeit based on the relatively few compounds tested, it appears that there was neither a bias for any particular killing speed nor significant correlation between speed of action and the previously quoted in vitro efficacy against *Pf*NF54.

Mechanistic Studies: Due to their structural likeness to CQ, which includes a planar heterocyclic moiety, a halo-substitution and a basic amine side group, the mechanistic potential of these compounds to inhibit Hz formation was investigated by measuring their ability to inhibit in vitro β-hematin (βH) formation. Although a number of these derivatives were able to inhibit βH formation (IC_{50} <100 μM) in a detergent-mediated Nonidet P-40 (NP-40) assay (Supporting Information **Table S1**), there was only a weak, albeit statistically significant, linear correlation with whole-cell activity against *Pf*NF54 (**Figure 5**). It is possible that the cell-free βH inhibition assay does not mirror the cellular Hz inhibitory activity or that there is only weak drug-haem complex formation due to poor binding to free haem molecules, or that Hz inhibition is not the sole target of this class of compounds.

To confirm if these compounds were bona-fide inhibitors of Hz formation, a cellular fractionation assay was used to determine free haem and Hz signatures when synchronized ring stage parasites were treated with increasing doses; for true inhibitors there is a dose-dependent increase in toxic free haem and corresponding decreases in Hz.[19] Of the cross section of compounds studied **8**, **9**, **54**, **45** were βH inhibitors in the NP-40 assay ($BHIA_{IC50} < 45\mu M$), whilst the inactive **69** ($BHIA_{IC50} = 120\mu M$) represented a negative control. No significant changes in toxic free haem or Hz levels with increasing drug concentrations were observed for **69** (**Figure 6**), whilst **8** and **45** showed significant concentration-dependent increases in free haem and corresponding decreases in haemozoin compared to the untreated control, with the free haem and parasite survival curves crossing close to the IC_{50} values of the compounds (**Figure 6**) - a trend not shown by **9** or **54** despite their potency in the NP-40 assay (Supporting Information **Figure S1**). In silico simulations of vacuolar accumulation of these compounds showed that they are likely to accumulate poorly within the digestive vacuole compared to standard haemozoin inhibitors (Supporting Information **Table S1**). Taken together, these studies suggest that inhibition of haemozoin formation is one but perhaps not the sole or primary target of this class of compounds; their flat conformation possibly allows for weak haem-drug complex formation through only π-π interactions as was recently reported for certain benzamide analogues.[20] This would be unlike halofantrine and quinine, for instance, which reportedly require hydrogen bonding and coordination to Fe(III)PPIX in addition to π–π interactions.[21, 22] The lack of βH inhibition by **69** could be ascribed to disrupted planarity (from the 2-F substitution) which potentially minimizes π–π interaction.

This leaves the intriguing prospect that the PBIs could act, at least in part, through an as yet unidentified mechanism. Amongst the diverse activities reported for other pyrido[1,2-*a*]benzimidazoles is the inhibition of the pore-forming protein perforin in mammalian cells by 1-amino-2, 4-dicyanopyrido[1,2-*a*]benzimidazoles.[23] This is interesting as the *P. falciparum* proteome harbors perforin-like proteins (PLPs) known to be involved in permeabilizing the erythrocyte membrane during egress of either gametocytes or merozoites.[24] An hydroxy derivative 2-Ethyl-1-hydroxy-3-methyl-pyrido[1,2-a]benzimidazole-4-carbonitrile (GNF7686) with potent in vitro activity against *Trypanosoma cruzi*, was also recently shown to act through inhibition of cytochrome b (a component of cytochrome bc1 or complex III),[25] and a well-established antimalarial target. Whilst the related hydroxy intermediates from our studies did not show significant antiplasmodial activity (unpublished data), this potential target warrants further investigation as a possible mode of action and encourages further testing for potential activity against kinetoplastids, including *Leishmania donovani*.

CONCLUSIONS

Further SAR studies, aided by physicochemical evaluation and microsomal stability studies, on the antimalarial activity of pyrido[1,2-*a*] benzimidazoles have led to a number of compounds with improved in vitro activity against *P. falciparum*, with substitution on the benzimidazole phenyl being a key factor in improving in vitro activity. Amongst the most active compounds in vitro, **59** and **60** showed significantly better in vivo activity in the mouse *P. berghei* model. The most active compounds also showed good activity against gametocytes, indicative of potential as dual-acting antimalarials. Other analogues have shown activity against the liver stage of *P.*

berghei. There is no conclusive evidence for their mode of action, although inhibition of haemozoin formation is identified as a potential contributory factor.

EXPERIMENTAL SECTION

All commercially available chemicals were purchased from either Sigma-Aldrich or Combi-Blocks. All solvents were dried by appropriate techniques. Unless otherwise stated, all solvents used were anhydrous. ^{1}H NMR spectra were recorded on a Varian Mercury Spectrometer at 300 MHz or a Varian Unity Spectrometer at 400 MHz.^{13}C NMR spectra were recorded at 75 MHz on a Varian Mercury Spectrometer or at 100 MHz on Varian Unity Spectrometer. Chemical shifts (δ) are given in ppm downfield from TMS as the internal standard. Coupling constants, *J*, are recorded in Hertz (Hz). High-resolution mass spectra were recorded on a VG70 SEQ micromass spectrometer. Melting points (m.pt) were determined by Differential Scanning Calorimetry (DSC) using TA Q200/Q2000 DSC from TA Instruments. Analytical thin-layer chromatography (TLC) was performed on aluminium-backed silica-gel 60 F_{254} (70-230 mesh) plates. Column chromatography was performed with Merck silica-gel 60 (70-230 mesh). Purity was determined by HPLC and all compounds were confirmed to have > 95% purity. The data that is not shown below is supplied in the Supporting Information.

General procedure for the synthesis of compound 4

A mixture of the substituted diaminobenzene 3(10 equiv.) and ethylcyanoacetate (2.0 equiv.) in DMF (1 mL) was heated in a microwave reactor at 110 °C for 15–45 min. The reaction mixture was then diluted with ethyl acetate (20 mL) and washed with water (3×15 ml). The organic phase was separated, dried over $MgSO_4$, filtered, solvent removed under reduced pressure and purified through column chromatography using MeOH: DCM as eluent to afford compound **4**.

2-(4-Chloro-1H-benzo[d]imidazol-2-yl)acetonitrile **4b**:

Yellow solid (49%). R_f 0.5 (65% EtOAc-Hexane). mp 190–192 ^{o}C. ^{1}H NMR (400 MHz, DMSO-d_6) δ 7.21 (m, 3H), 5.20 (br s, 1H), 3.89 (s, 2H). ^{13}C NMR (100 MHz, DMSO-d_6) δ 146.3, 140.0, 136.1, 127.3, 125.7, 123.8, 121.9, 116.8, 116.4. MS: LC-MS: $(ESI)^{+}$: found *m/z* 191.2[M^{+}]:193.4[M+2]$^{+}$(3:1), (calculated for $C_9H_6ClN_3$: 191.62).

2-(3H-imidazo[4,5-*b*]pyridin-2-yl)acetonitrile **4i**:

Brown solid (97%). R_f 0.3 (10% MeOH-DCM). mp 172–174 ^{o}C. ^{1}H NMR (400 MHz, DMSO-d_6) δ 13.17 (br s, 1H), 8.34 (m, 1H), 7.99 (m, 1H), 7.24 (m, 1H), 4.45 (s, 2H). ^{13}C NMR (100 MHz, DMSO-d_6) δ 147.6, 144.2 (2C), 127.2, 118.5 (2C), 116.6, 19.2. MS: LC-MS: $(ESI)^{+}$: found *m/z* 159.2 $[M+H]^{+}$, (calculated for $C_8H_6N_4$: 158.16).

General procedure for the synthesis of compound 5

A mixture of benzimidazole acetonitrile **4** (1.0 equiv.), NH_4OAc (2.0 equiv.), and the appropriate *β*-keto ester 2 (1.20 equiv.) was heated to reflux at 150^{o}C for 1h and then allowed to cool to 100 ^{o}C. MeCN (10 mL) was added and the resulting mixture stirred for 15 min, allowed to cool to room temperature and then cooled on ice. The cold mixture was filtered and the residue washed with cold MeCN (4×10 mL), dried in vacuo, and used in the next step without further purification.

3-(3,4-dichlorophenyl)-1-hydroxybenzo[4,5]imidazo[1,2-*a*]pyridine-4-carbonitrile **5i**:

Silver tan powder (75%). R_f 0.7 (70% EtOAc-Hexane). mp 249–251 ^{o}C. ^{1}H NMR (400 MHz, DMSO-d_6) δ 13.80 (br s, 1H), 8.61 (d, J = 8.1 Hz, 1H), 7.90 (d, J = 2.1 Hz, 1H), 7.82 (d, J = 8.1 Hz, 1H), 7.64 (dd, J = 8.3, 2.2 Hz, 1H), 7.58 (m, 2H), 7.41 (t, J = 8.2 Hz, 1H), 6.10 (s, 1H). ^{13}C

NMR (100 MHz, DMSO-d_6) δ 158.5, 150.2, 147.9, 137.9, 132.8, 132.5 (2C), 131.9, 131.3, 130.5, 129.0, 128.1, 127.3, 123.1, 117.0, 116.7, 112.2, 105.0. MS: LC-MS: $(ESI)^+$: found *m/z* 354.1$[M^+]$:356.2$[M+2]^+$(3:1), (calculated for $C_{18}H_9Cl_2N_3O$: 354.19).

7,8-Dichloro-1-hydroxy-3-(4-(trifluoromethyl)phenyl)benzo[4,5]imidazo[1,2-*a*]pyridine-4-carbonitrile **5t**:

Brownish solid (74%). R_f 0.3 (70% EtOAc-Hexane). mp 305–307 ^oC. ^1H NMR (600 MHz, DMSO-d_6) δ 8.63 (s, 1H), 7.90 (d, *J* = 8.2 Hz, 2H), 7.83 (d, *J* = 8.1 Hz, 2H), 7.72 (s, 1H), 6.02 (s, 1H). ^{13}C NMR (150 MHz, DMSO-d_6) δ 158.5, 151.8, 150.0, 141.7, 130.0, 129.6 (2C), 129.1, 128.1 (2C), 126.0, 125.9, 125.4, 124.0, 123.6, 117.2 (2C), 114.1, 104.2. MS: LC-MS: $(ESI)^+$: found *m/z* 422.1$[M^+]$:424.3$[M+2]^+$:426.4$[M+4]^+$(9:3:1), (calculated for $C_{19}H_8Cl_2F_3N_3O$: 422.19).

General procedure for the synthesis of compound 6

A mixture of compound **5** (1.0 equiv.) and $POCl_3$ (20 equiv.) was heated to reflux at 130 ^oC for 2 h. Excess $POCl_3$ was removed under reduced pressure and ice-cold water (20 mL) added to the residue, stirring to yield a precipitate. The mixture was neutralized with saturated $NaHCO_3$ and filtered. The resultant solid was washed with ice-cold water (4×15 mL), dried in vacuo, and used without further purification.

1-Chloro-3-(3,4-dichlorophenyl)benzo[4,5]imidazo[1,2-*a*]pyridine-4-carbonitrile **6i**:

Yellow solid (98%). R_f 0.6 (30% EtOAc-Hexane). mp 260–262 ^oC. ^1H NMR (400 MHz, DMSO-d_6) δ 8.72 (d, *J* = 8.1 Hz, 1H), 8.09 (s, 1H), 8.03 (d, *J* = 2.1 Hz, 1H), 7.90 (d, *J* = 8.1 Hz, 1H), 7.83 (dd, *J* = 8.3, 2.2 Hz, 1H), 7.73 (t, *J* = 2.1 Hz, 1H), 7.62 (d, *J* = 2.1 Hz, 1H), 7.44 (t, *J* = 8.2 Hz, 1H). ^{13}C NMR (100 MHz, DMSO-d_6) δ 159.5, 152.2, 148.5, 136.7, 132.7, 132.1 (2C),

131.7, 131.2, 130.1, 129.5, 128.8, 127.5, 123.9, 118.1, 116.5, 113.2, 106.0. MS: LC-MS: $(ESI)^+$: found *m/z* 372.4$[M^+]$:374.3$[M+2]^+$:376.4$[M+4]^+$(9:3:1), (calculated for $C_{18}H_8Cl_3N_3$: 372.63).

1,7,8-Trichloro-3-(4-(trifluoromethyl)phenyl)benzo[4,5]imidazo[1,2-*a*]pyridine-4-carbonitrile **6t**:

Brownish solid (97%). R_f 0.8 (70% EtOAc-Hexane). mp. 253–255 ^oC. ^1H NMR (600 MHz, DMSO-d_6) δ 8.86 (s, 1H), 8.34 (s, 1H), 8.03 (m, 4H), 7.70 (s, 1H). ^{13}C NMR (150 MHz, DMSO-d_6) δ 149.5, 149.4, 144.3, 139.1, 135.4, 134.7, 130.9, 130.4, 130.2, 128.9, 126.4 (2C), 125.2, 125.1, 123.4, 121.2, 117.5, 115.0, 113.6; MS: LC-MS: $(ESI)^+$: found *m/z* 440 $[M]^+$: 442.6 $[M+2]^+$:444 $[M+4]^+$ (9:3:1), (calculated for $C_{19}H_7Cl_3N_3$: 440.63).

General procedure for the synthesis of compounds 8 - 69

Amine (2.0 equiv.) was added to a stirred mixture of compound **6/7a-b** (1.0 equiv.) and triethylamine (2.0 equiv.) in THF (10 mL). The mixture was irradiated in microwave reactor at 80^{o}C for 20 min., filtered hot, and allowed to cool. The solvent was removed in vacuo, and the residue washed with minimum amount of ice-cold ethanol. The resulting solid was recrystallized from acetone or ethanol to afford the target compound.

1-((2-(3-Hydroxypyrrolidin-1-yl)ethyl)amino)-3-(4-(trifluoromethyl)phenyl)benzo[4,5]imidazo[1,2-*a*]pyridine-4-carbonitrile **11**:

Yellow solid (53%). R_f 0.3 (8% MeOH-DCM). mp 267–269 ^oC. ^1H NMR (600 MHz, DMSO-d_6) δ 8.39 (d, *J* = 8.4 Hz, 1H), 7.98 (d, *J* = 9.1 Hz, 2H), 7.98 (d, *J* = 9.1 Hz, 2H), 7.87 (d, *J* = 8.1 Hz, 1H), 7.58 (t, *J* = 8.1 Hz, 1H), 7.39 (t, *J* = 8.1 Hz, 1H), 6.28 (s, 1H), 4.80 (br s, 1H), 4.27 (m, 1H), 3.65 (t, *J* = 6.2 Hz, 2H), 2.90 (m, 2H), 2.84 (m, 2H), 2.58 (m, 2H), 2.07 (m, 1H), 1.64 (m, 1H).^{13}C NMR (150 MHz, DMSO-d_6) δ 150.6, 149.3, 149.0, 145.4, 141.8, 130.3, 130.0, 128.3,

126.4, 126.0, 125.4 (2C), 123.6 (2C), 121.2, 119.0, 117.6, 114.8, 90.7, 69.8, 62.8, 53.3, 52.5, 41.8,34.9. LC-MS: $(ESI)^+$: found *m/z* =466.1 $[M+H]^+$, (calculated for $C_{25}H_{22}F_3N_5O$: 465.48).HPLC purity 99% (t_r = 4.09 min).

1-((5-(Diethylamino)pentan-2-yl)amino)-3-(4-(trifluoromethyl)phenyl)benzo[4,5]imidazo[1,2-*a*]pyridine-4-carbonitrile **17**:

Yellow solid (50%). R_f 0.3 (10% MeOH-DCM). mp 220–222 °C. ^{1}H NMR (400 MHz, DMSO-d_6) δ 8.42 (d, *J* = 8.3 Hz, 1H), 7.96 (m, 4H), 7.85 (d, *J* = 8.0 Hz, 1H), 7.58 (t, *J* = 7.7 Hz, 1H), 7.39 (t, *J* = 7.3 Hz, 1H), 6.31 (s, 1H), 4.03 (m, 1H), 2.48 (m, 6H), 1.92 (m, 1H), 1.65 (m, 3H), 1.38 (d, *J* = 6.3 Hz, 3H), 0.91 (t, *J* = 7.0 Hz, 6H).^{13}C NMR (100 MHz, DMSO-d_6) δ 150.5, 149.6, 149.1(2C), 145.4, 142.0, 130.3, 130.0 (2C), 128.6, 126.3, 126.0 (2C), 123.1, 120.6, 118.8, 117.6, 115.8, 91.3, 52.1, 50.0, 46.6 (2C), 33.7, 23.5, 20.1 (2C), 11.5.LC-MS: $(ESI)^+$: found *m/z* =494.4 $[M+H]^+$, (calculated for $C_{28}H_{30}F_3N_5$: 493.58).HPLC purity98% (t_r = 3.69 min).

1-((N-Methylpiperidin-4-yl)amino)-3-(4-(trifluoromethyl)phenyl)benzo[4,5]imidazo[1,2-*a*]pyridine-4-carbonitrile **20**:

Yellow solid (51%). R_f 0.4 (10% MeOH-DCM). mp 215–217 ºC.^{1}H NMR (400 MHz, DMSO) δ 8.41 (d, *J* = 8.3 Hz, 1H), 7.96 (s, 4H), 7.85 (d, *J* = 8.1 Hz, 1H), 7.58 (t, *J* = 7.7 Hz, 1H), 7.40 (t, *J* = 7.4 Hz, 1H), 6.34 (s, 1H), 3.83 (m, 1H), 2.84 (m, 2H), 2.24 (s, 3H), 2.17 (t, *J* = 10.6 Hz, 2H), 2.07 (m, 2H), 1.92 (t, *J* = 9.6 Hz, 2H).^{13}C NMR (101 MHz, DMSO) δ 150.6, 149.6, 148.9, 145.4, 142.0, 141.9, 130.3, 130.2, 130.0, 128.7, 128.6, 126.4, 126.2, 126.1, 126.0, 120.7, 118.8, 117.7, 117.6, 116.1, 91.6, 54.4, 50.7, 46.3, 31.1. LC-MS: $(ESI)^+$: found *m/z* =450.2 $[M+H]^+$, (calculated for $C_{25}H_{22}F_3N_5$: 449.48).HPLC purity 99% (t_r = 4.03 min).

3-(3,4-Dichlorophenyl)-1-((2-(ethylamino)ethyl)amino)benzo[4,5]imidazo[1,2-*a*]pyridine-4-carbonitrile **45**:

Yellow solid (29%). R_f 0.1 (5% MeOH/DCM). mp 235–237 °C. ^{1}H NMR (400 MHz, DMSO-d_6) δ 8.52 (d, J = 8.1 Hz, 1H), 7.96 (s, 1H), 7.83 (d, J = 8.3 Hz, 1H), 7.77 (d, J = 7.9 Hz, 1H), 7.71 (d, J = 8.0 Hz, 1H), 7.50 (t, J = 7.6 Hz, 1H), 7.30 (t, J = 7.5 Hz, 1H), 6.12 (s, 1H), 3.64 (t, J = 6.2 Hz, 2H), 3.07 (t, J = 5.6 Hz, 2H), 2.80 (q, J = 8.0 Hz, 2H), 1.13 (t, J = 7.0 Hz, 3H).^{13}C NMR (100 MHz, DMSO-d_6) δ 150.0, 148.5, 145.4, 138.9, 132.5, 131.8, 131.1, 130.9, 129.3, 129.0 (2C), 125.7, 120.3, 118.5, 118.3 (2C), 115.4, 90.5, 47.2, 43.1, 43.1, 14.3.LC-MS: $(ESI)^+$: found m/z =424.2$[M^+]$:426.5$[M+2]^+$(3:1), (calculated for $C_{22}H_{19}Cl_2N_5$: 424.33).HPLC purity 99% (t_r = 3.53 min).

9-Chloro-1-((2-(ethylamino)ethyl)amino)-3-(4-(trifluoromethyl)phenyl)benzo[4,5]imidazo[1,2-*a*]pyridine-4-carbonitrile **57**:

Yellow solid (36%). R_f 0.2 (6% MeOH-DCM). mp 223–225 °C. ^{1}H NMR (400 MHz, DMSO-d_6) δ 8.69 (d, J = 8.7 Hz, 1H), 7.90 (m, 4H), 7.44 (d, J = 7.4 Hz, 1H), 7.13 (t, J = 8.0 Hz, 1H), 5.83 (s, 1H), 3.58 (t, J = 6.2 Hz, 2H), 3.18 (t, J = 6.2 Hz, 2H), 2.94 (q, J = 7.2 Hz, 2H), 1.18 (t, J = 7.2 Hz, 3H). ^{13}C NMR (100 MHz, DMSO-d_6) δ 152.2, 151.9, 148.6, 143.5, 142.5, 131.5, 129.7, 129.4, 126.0, 125.8, 125.7, 124.2, 123.3, 120.3, 120.1, 119.5, 115.4 (C2), 72.8, 48.0, 44.4, 43.0, 12.9.LC-MS: $(ESI)^+$: found m/z =458.3$[M^+]$:460.5$[M+2]^+$(3:1), (calculated for $C_{23}H_{19}ClF_3N_5$: 457.89).HPLC purity 98% (t_r = 3.52 min).

7,8-Dichloro-1-((2-(ethylamino)ethyl)amino)-3-(4-(trifluoromethyl)phenyl)benzo[4,5]imidazo[1,2-*a*]pyridine-4-carbonitrile **59**:

Yellow solid (47%). R_f 0.4 (8% MeOH-DCM). mp 266–268 °C. ^{1}H NMR (600 MHz, DMSO-d_6) δ 8.92 (s, 1H), 7.85 (d, J = 8.8 Hz, 2H), 7.84 (d, J = 8.4 Hz, 2H), 7.72 (s, 1H), 5.72 (s, 1H), 3.60 (t, J = 6.2 Hz, 2H), 3.23 (t, J = 6.2 Hz, 2H), 3.03 (q, J = 7.3 Hz, 2H), 1.24 (t, J = 7.3 Hz, 3H).^{13}C NMR (150 MHz, DMSO-d_6) δ 154.1, 152.4, 148.1, 145.5, 143.8, 130.2, 129.6 (2C),

129.5, 129.3, 126.3, 125.6, 123.7, 120.3, 119.9, 117.6 (2C), 116.7, 91.6, 48.1, 44.7, 42.9, 12.2.LC-MS: $(ESI)^+$: found *m/z* =492.2$[M^+]$:494.4$[M+2]^+$:496.5$[M+4]^+$(9:3:1), (calculated for $C_{23}H_{18}Cl_2F_3N_5$: 492.33).HPLC purity 98% (t_r = 4.29 min).

7,9-Dichloro-1-((2-(ethylamino)ethyl)amino)-3-(4-(trifluoromethyl)phenyl)benzo[4,5]imidazo[1,2-*a*]pyridine-4-carbonitrile **60**:

Yellow solid (42%). R_f 0.3 (8% MeOH-DCM). mp 277–279 ^oC. ^1H NMR (600 MHz, DMSO-d_6) δ 8.81 (d, *J* = 2.0 Hz, 1H), 7.86 (d, *J* = 8.4 Hz, 2H), 7.83 (d, *J* = 8.2 Hz, 2H), 7.43 (d, *J* = 2.0 Hz, 1H), 5.67 (s, 1H), 3.57 (t, *J* = 6.2 Hz, 2H), 3.26 (t, *J* = 6.2 Hz, 2H), 3.06 (q, *J* = 7.2 Hz, 2H), 1.24 (t, *J* = 7.2 Hz, 3H).^{13}C NMR (150 MHz, DMSO-d_6) δ 153.9, 152.9, 147.7, 144.0, 141.6, 132.2, 129.6 (2C), 129.2, 125.7, 125.6, 123.7 (2C), 123.1, 121.8, 120.8, 119.6, 115.6, 91.9, 48.1, 44.9, 42.7, 11.8.LC-MS: $(ESI)^+$: found *m/z* =492.2$[M^+]$:494.4$[M+2]^+$:496.5$[M+4]^+$(9:3:1), (calculated for $C_{23}H_{18}Cl_2F_3N_5$: 492.33).HPLC purity 99% (t_r = 4.26 min).

6-((2-(Ethylamino)ethyl)amino)-8-(4-(trifluoromethyl)phenyl)imidazo[1,2-*a*:4,5-*b*']dipyridine-9-carbonitrile **64**:

Yellow solid (32%). R_f 0.3 (10% MeOH-DCM). mp 225–227 ^oC. ^1H NMR (400 MHz, DMSO-d_6) δ 8.41 (dd, *J* = 4.8, 1.4 Hz, 1H), 8.26 (dd, *J* = 8.2, 1.4 Hz, 1H), 7.95 (m, 4H), 7.64 (dd, *J* = 8.2, 4.8 Hz, 1H), 6.33 (s, 1H), 3.67 (t, *J* = 6.0 Hz, 2H), 2.94 (t, *J* = 6.0 Hz, 2H), 2.65 (q, *J* = 7.1 Hz, 2H), 1.08 (t, *J* = 7.1 Hz, 3H). ^{13}C NMR (100 MHz, DMSO-d_6) δ 152.3, 149.2, 149.0, 144.1, 141.9, 140.3, 137.8, 130.4, 130.0 (2C), 126.5, 126.0 (2C), 122.2 (3C), 117.3, 90.1, 47.4, 43.5, 42.7, 15.6. LC-MS: $(ESI)^+$: found *m/z* =425.2$[M+1]^+$, (calculated for $C_{22}H_{19}F_3N_6$: 424.43).HPLC purity 96% (t_r = 3.25 min).

2-Fluoro-1-((2-(3-hydroxypyrrolidin-1-yl)ethyl)amino)-3-(4-(trifluoromethyl)phenyl)benzo[4,5]imidazo[1,2-*a*]pyridine-4-carbonitrile **69**:

Yellow solid (44%). R_f 0.3 (5% MeOH-DCM). mp. 265–267 °C.^{1}H NMR (400 MHz, DMSO-*d*6) δ 8.54 (d, *J* = 8.4 Hz, 1H), 7.96 (d, *J* = 8.0 Hz, 2H), 7.86 (d, *J* = 8.0 Hz, 2H), 7.82 (d, *J* = 8.2 Hz, 1H), 7.55 (t, *J* = 7.8 Hz, 1H), 7.34 (t, *J* = 7.8 Hz, 1H), 4.30 (m, 1H), 3.87 (m, 2H), 2.98 (m, 2H), 2.92 (m, 2H), 2.69 (m, 2H), 2.10 (m, 1H), 1.70 (m, 1H). ^{13}C NMR (100 MHz, DMSO-*d*6) δ 147.2, 145.6, 141.3, 141.0, 136.5, 133.0, 130.9, 130.1, 130.1, 126.1, 125.8, 125.8, 120.6, 118.7, 117.2, 117.1, 115.5, 69.8, 62.5, 55.4, 55.3, 52.4, 44.3, 44.2, 34.7. LC-MS: $(ESI)^+$: found *m/z* = 484.2 [M+H]+, (calculated for $C_{25}H_{21}F_4N_5O$: 483.17). HPLC purity 99% (t_r = 3.51 min).

ASSOCIATED CONTENT

Supporting Information

Characterization of all intermediates as well as final compounds, details of assay procedures and further descriptions of the biological experiments (cytotoxicity analysis, *in vitro* determination of antiplasmodial activity, *in vivo* efficacy experiments, *in vitro* gametocytocidal experiments, liver stage assays and killing kinetics), *in vitro* ADME assays (kinetic solubility and artificial membrane permeability experiments), metabolic stability experiments and determination of mechanism of action (*in vitro* β-haematin, haem fractionation assays and prediction of vacuolar accumulation) are available in the Supporting Information section at http://pubs.acs.org.

AUTHOR INFORMATION

Corresponding author

* Phone: +27-21-6502557. Fax: +27-21-6505195. E-mail: Kelly.Chibale@uct.ac.za

ACKNOWLEDGEMENT

The University of Cape Town, South African Medical Research Council (SAMRC), and South African Research Chairs Initiative of the Department of Science and Technology, administered through the South African National Research Foundation are gratefully acknowledged for support (K.C.). The SAMRC is further acknowledged for support (L-MB, T.L.C, and T.J.E.).

ABBREVIATIONS

SAR, structure-activity relationships; ADME, absorption, distribution, metabolism and excretion; CQ, chloroquine; p.o., oral administration; i.v., intravenous administration; MSD, mean survival days; PK, pharmacokinetics; PBIs, pyrido[1,2-*a*]benzimidazoles; BHIA, beta-haematin inhibition assay; LG, late gametocytes; EG, early gametocytes.

REFERENCES

1. World Health Organization (WHO). *World Malaria Report 2015.* *http://www.who.int/malaria/publications/world_malaria_report_2015/wmr-2015-no-profiles.pdf?ua=1*; Geneva, Switzerland (accessed 24th September 2016).

2. Prudencio, M.; Rodriguez, A.; Mota, M. M. The Silent Path to Thousands of Merozoites: The *Plasmodium* Liver Stage. *Nat. Rev. Microbiol.* **2006,** *4*, 849-856.

3. Dondorp, A. M.; Nosten, F.; Yi, P.; Das, D.; Phyo, A. P.; Tarning, J.; Lwin, K. M.; Ariey, F.; Hanpithakpong, W.; Lee, S. J.; Ringwald, P.; Silamut, K.; Imwong, M.; Chotivanich, K.; Lim, P.; Herdman, T.; An, S. S.; Yeung, S.; Singhasivanon, P.; Day, N. P.; Lindegardh, N.; Socheat, D.; White, N. J. Artemisinin Resistance in *Plasmodium falciparum* Malaria. *N. Engl. J. Med.* **2009,** *361*, 455-467.

4. Noedl, H.; Se, Y.; Schaecher, K.; Smith, B. L.; Socheat, D.; Fukuda, M. M. Evidence of Artemisinin-resistant Malaria in western Cambodia. *N. Engl. J. Med.* **2008,** *359*, 2619-2620.

5. Horton, D. A.; Bourne, G. T.; Smythe, M. L. The Combinatorial Synthesis of Bicyclic Privileged Structures or Privileged Substructures. *Chem. Rev.* **2003,** *103*, 893-930.

6. Camacho, J.; Barazarte, A.; Gamboa, N.; Rodrigues, J.; Rojas, R.; Vaisberg, A.; Gilman, R.; Charris, J. Synthesis and Biological Evaluation of Benzimidazole-5-carbohydrazide Derivatives as Antimalarial, Cytotoxic and Antitubercular Agents. *Bioorg. Med. Chem.* **2011,** *19*, 2023-2029.

7. Keri, R. S.; Hiremathad, A.; Budagumpi, S.; Nagaraja, B. M. Comprehensive Review in Current Developments of Benzimidazole-Based Medicinal Chemistry. *Chem. Biol. Drug. Des.* **2015,** *86*, 19-65.

8. Keurulainen, L.; Vahermo, M.; Puente-Felipe, M.; Sandoval-Izquierdo, E.; Crespo-Fernandez, B.; Guijarro-Lopez, L.; Huertas-Valentin, L.; de las Heras-Duena, L.; Leino, T. O.; Siiskonen, A.; Ballell-Pages, L.; Sanz, L. M.; Castaneda-Casado, P.; Jimenez-Diaz, M. B.; Martinez-Martinez, M. S.; Viera, S.; Kiuru, P.; Calderon, F.; Yli-Kauhaluoma, J. A Developability-Focused Optimization Approach Allows Identification of in Vivo Fast-Acting Antimalarials: N-[3-[(Benzimidazol-2-yl)amino]propyl]amides. *J. Med. Chem.* **2015,** *58*, 4573-4580.

9. Saify, Z. S.; Azim, M. K.; Ahmad, W.; Nisa, M.; Goldberg, D. E.; Hussain, S. A.; Akhtar, S.; Akram, A.; Arayne, A.; Oksman, A.; Khan, I. A. New Benzimidazole Derivatives as Antiplasmodial Agents and Plasmepsin Inhibitors: Synthesis and Analysis of Structure-Activity Relationships. *Bioorg. Med. Chem. Lett.* **2012,** *22*, 1282-1286.

10. Rida, S.; Farid, S.; El-Sayed, B. B.; El-Ghazzawi, E.; Kader, O.; Kappe, T. Benzimidazole Condensed Ring Systems. 1. Syntheses and Biological Investigations of Some Substituted Pyrido[1,2-a]benzimidazoles. *J. Heterocycl. Chem.* **1988,** *25*, 1087-1093.

11. Ndakala, A. J.; Gessner, R. K.; Gitari, P. W.; October, N.; White, K. L.; Hudson, A.; Fakorede, F.; Shackleford, D. M.; Kaiser, M.; Yeates, C.; Charman, S. A.; Chibale, K. Antimalarial Pyrido[1,2-a]benzimidazoles. *J. Med. Chem.* **2011,** *54*, 4581-4589.

12. Ishikawa, M.; Hashimoto, Y. Improvement in Aqueous Solubility in Small Molecule Drug Discovery Programs by Disruption of Molecular Planarity and Symmetry. *J. Med. Chem.* **2011,** *54*, 1539-1554.

13. Reader, J.; Botha, M.; Theron, A.; Lauterbach, S. B.; Rossouw, C.; Engelbrecht, D.; Wepener, M.; Smit, A.; Leroy, D.; Mancama, D.; Coetzer, T. L.; Birkholtz, L. M. Nowhere to Hide: Interrogating Different Metabolic Parameters of *Plasmodium falciparum* Gametocytes in a Transmission-blocking Drug Discovery Pipeline Towards Malaria Elimination. *Malar. J.* **2015,** *14*, 213.

14. Prudencio, M.; Mota, M. M.; Mendes, A. M. A Toolbox to Study Liver Stage Malaria. *Trends. Parasitol.* **2011,** *27*, 565-574.

15. Ploemen, I. H.; Prudencio, M.; Douradinha, B. G.; Ramesar, J.; Fonager, J.; van Gemert, G. J.; Luty, A. J.; Hermsen, C. C.; Sauerwein, R. W.; Baptista, F. G.; Mota, M. M.; Waters, A. P.; Que, I.; Lowik, C. W.; Khan, S. M.; Janse, C. J.; Franke-Fayard, B. M. Visualisation and Quantitative Analysis of the Rodent Malaria Liver Stage by Real Time Imaging. *PLoS One* **2009,** *4*, e7881.

16. Carrasco, M. P.; Machado, M.; Goncalves, L.; Sharma, M.; Gut, J.; Lukens, A. K.; Wirth, D. F.; Andre, V.; Duarte, M. T.; Guedes, R. C.; Dos Santos, D. J.; Rosenthal, P. J.; Mazitschek,

R.; Prudencio, M.; Moreira, R. Probing the Azaaurone Scaffold against the Hepatic and Erythrocytic Stages of Malaria Parasites. *ChemMedChem* **2016,** *11*, 2194-2204.

17. Vale, N.; Moreira, R.; Gomes, P. Primaquine Revisited Six Decades After Its Discovery. *Eur. J. Med. Chem.* **2009,** *44*, 937-953.

18. Le Manach, C.; Scheurer, C.; Sax, S.; Schleiferbock, S.; Cabrera, D. G.; Younis, Y.; Paquet, T.; Street, L.; Smith, P.; Ding, X. C.; Waterson, D.; Witty, M. J.; Leroy, D.; Chibale, K.; Wittlin, S. Fast In Vitro Methods to Determine The Speed of Action and the Stage-specificity of Anti-malarials in *Plasmodium falciparum*. *Malar. J.* **2013,** *12*, 424-430.

19. Combrinck, J. M.; Mabotha, T. E.; Ncokazi, K. K.; Ambele, M. A.; Taylor, D.; Smith, P. J.; Hoppe, H. C.; Egan, T. J. Insights Into The Role of Heme in the Mechanism of Action of Antimalarials. *ACS Chem. Biol.* **2013,** *8*, 133-137.

20. Wicht, K. J.; Combrinck, J. M.; Smith, P. J.; Hunter, R.; Egan, T. J. Identification and SAR Evaluation of Hemozoin-inhibiting Benzamides Active Against *Plasmodium falciparum*. *J. Med. Chem.* **2016,** *59*, 6512-6530.

21. de Villiers, K. A.; Gildenhuys, J.; le Roex, T. Iron(III)Protoporphyrin IX Complexes of the Antimalarial Cinchona Alkaloids Quinine and Quinidine. *ACS Chem. Biol.* **2012,** *7*, 666-671.

22. de Villiers, K. A.; Marques, H. M.; Egan, T. J. The Crystal Structure of Halofantrine-Ferriprotoporphyrin IX and the Mechanism of Action of Arylmethanol Antimalarials. *J. Inorg. Biochem.* **2008,** *102*, 1660-1667.

23. Lyons, D. M.; Huttunen, K. M.; Browne, K. A.; Ciccone, A.; Trapani, J. A.; Denny, W. A.; Spicer, J. A. Inhibition of the Cellular Function of Perforin by 1-amino-2,4-dicyanopyrido[1,2-a]benzimidazoles. *Bioorg. Med. Chem.* **2011,** *19*, 4091-4100.

24. Wirth, C. C.; Glushakova, S.; Scheuermayer, M.; Repnik, U.; Garg, S.; Schaack, D.; Kachman, M. M.; Weissbach, T.; Zimmerberg, J.; Dandekar, T.; Griffiths, G.; Chitnis, C. E.; Singh, S.; Fischer, R.; Pradel, G. Perforin-like Protein PPLP2 Permeabilizes the Red Blood Cell Membrane During Egress of *Plasmodium falciparum* Gametocytes. *Cell. Microbiol.* **2014,** *16*, 709-733.

25. Khare, S.; Roach, S. L.; Barnes, S. W.; Hoepfner, D.; Walker, J. R.; Chatterjee, A. K.; Neitz, R. J.; Arkin, M. R.; McNamara, C. W.; Ballard, J.; Lai, Y.; Fu, Y.; Molteni, V.; Yeh, V.; McKerrow, J. H.; Glynne, R. J.; Supek, F. Utilizing Chemical Genomics to Identify Cytochrome b as a Novel Drug Target for Chagas Disease. *PLoS Pathog.* **2015,** *11*, e1005058.

26. Paquet, T.; Le Manach, C.; Cabrera, D. G.; Younis, Y.; Henrich, P.; Abraham, T.; Lee, M. C. S.; Basak, R.; Ghidelli-Disse, S.; Lafuente-Monasterio, M. J.; Bantscheff, M.; Ruecker, A.; Blagborough, A. M.; Zakutansky, S.; Zeeman, A.-M.; White, K. L.; Shackleford, D. M.; Mannila, J.; Morizzi, J.; Scheurer, C.; Angulo-Barturen, I.; Martínez, M. S.; Ferrer, S.; Sanz, L. M.; Gamo, F. J.; Reader, J.; Botha, M.; Dechering, K. J.; Sauerwein, R. W.; Tungtaeng, A.; Vanachayangkul, P.; Lim, C. S.; Burrows, J. N.; Witty, M. J.; Marsh, K. C.; Bodenreider, C.; Rochford, R.; Solapure, S. M.; Jiménez-Díaz, M. B.; Wittlin, S.; Charman, S. A.; Donini, C.; Campo, B.; Birkholtz, L.-M.; Hanson, K. K.; Drewes, G.; Kocken, C.; Delves, M. J.; Leroy, D.; Fidock, D. A.; Waterson, D.; Street, L. J.; Chibale, K. (In Press) Target Identification and Elucidation of the Complete Life Cycle Fingerprint of the Novel *Plasmodium* PI4K inhibitor MMV390048. *Sci. Transl. Med.* **2017**.

27. Le Manach, C.; Gonzalez Cabrera, D.; Douelle, F.; Nchinda, A. T.; Younis, Y.; Taylor, D.; Wiesner, L.; White, K. L.; Ryan, E.; March, C.; Duffy, S.; Avery, V. M.; Waterson, D.; Witty, M. J.; Wittlin, S.; Charman, S. A.; Street, L. J.; Chibale, K. Medicinal Chemistry

Optimization of Antiplasmodial Imidazopyridazine Hits From High Throughput Screening of a SoftFocus Kinase Library: Part 1. *J. Med. Chem.* **2014,** *57*, 2789-2798.

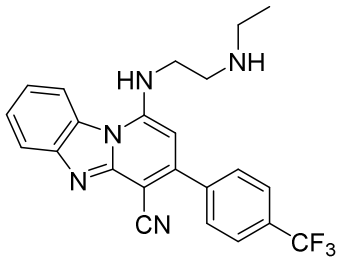

8

*Pf*NF54 = 0.11 μM

*Pf*K1 = 0.12 μM

in vivo *P. berghei* (HCl salt: p.o) 4×25 mg/kg = 95.7%

0/3 malaria infected mice cured

Figure 1: Original lead compound **8**, with activity against chloroquine-sensitive (*Pf*NF54) and chloroquine/multidrug-resistant (*Pf*K1) *P. falciparum* strains.[11]

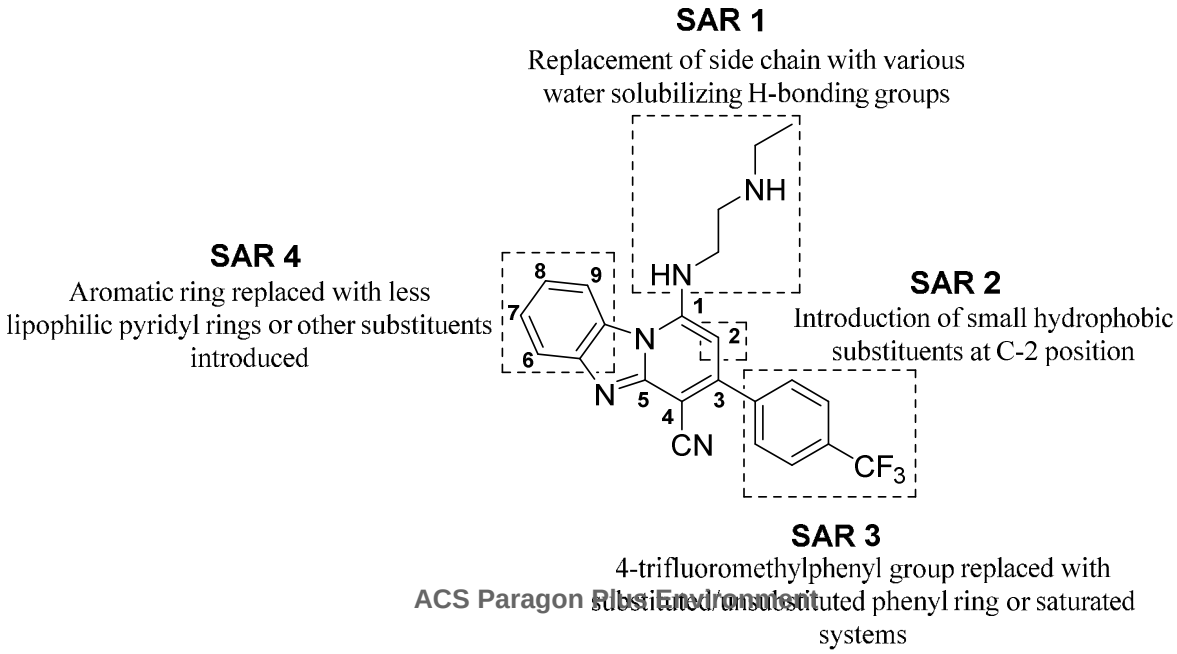

Figure 2: SAR explorations around lead compound **8**.

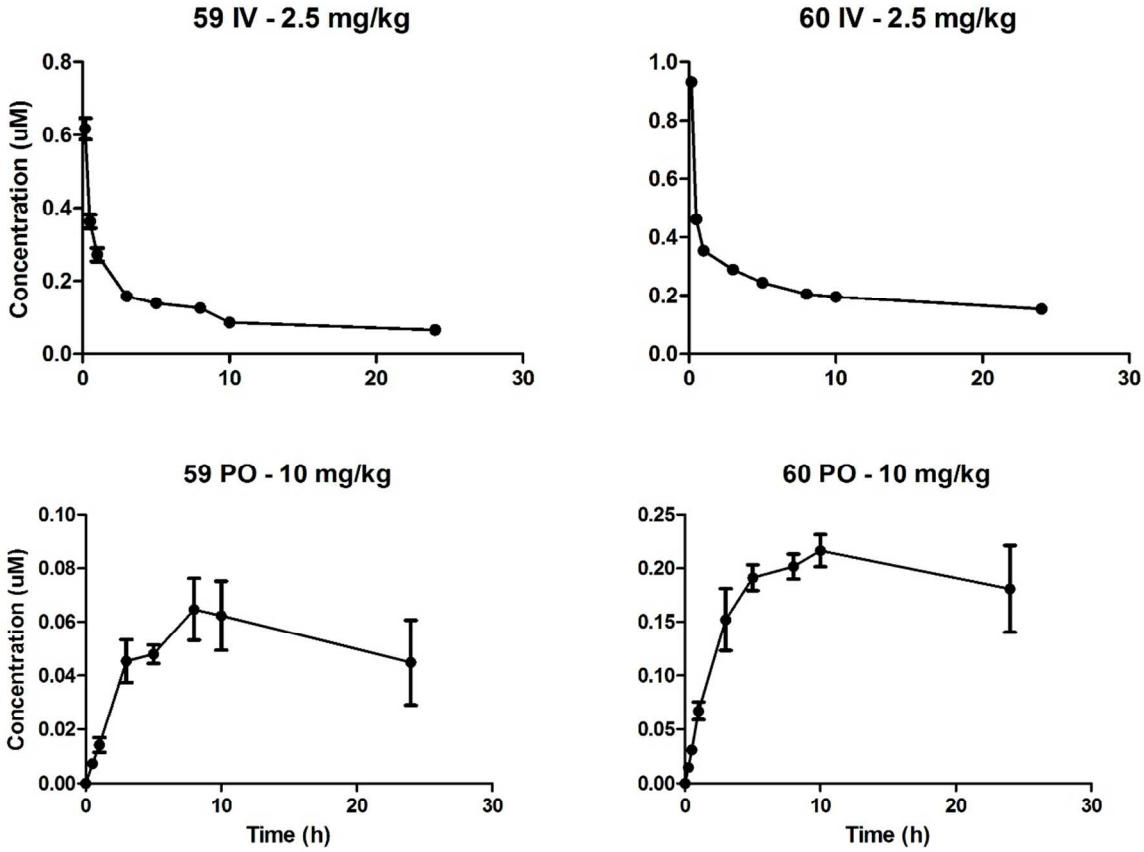

Figure 3: Systemic exposure of **59** and **60** following single intravenous and oral dose administration to healthy mice (n=3).

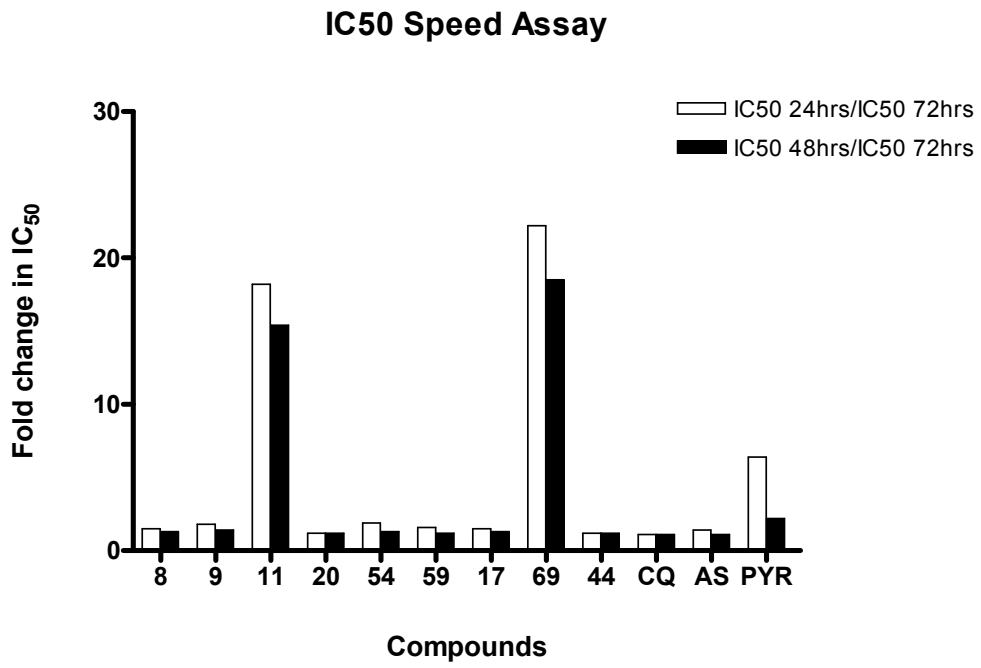

Figure 4: Change in activity of compounds at different assay durations relative to 72 h assay.

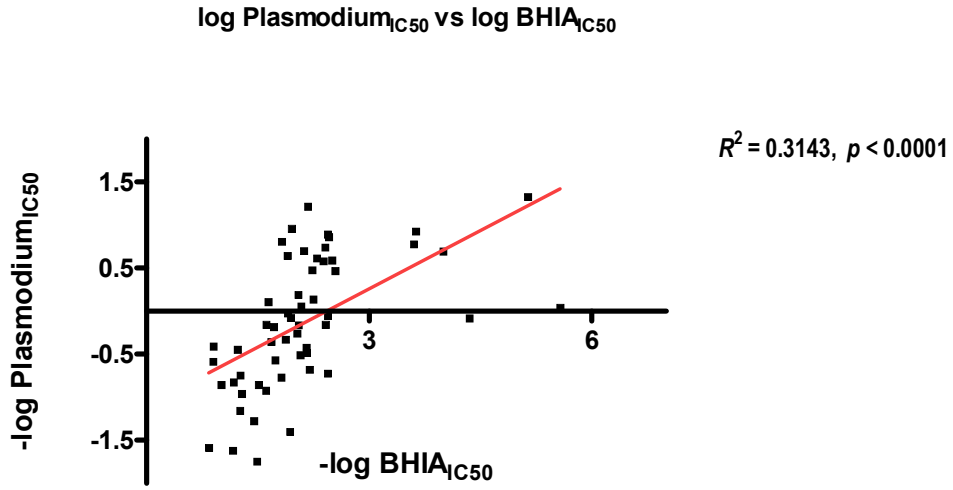

Figure 5: Linear correlation between the inverse of the βH and parasite growth IC_{50} values for *Pf*NF54. Measurements of βH and parasite growth inhibitions were both done in triplicates.

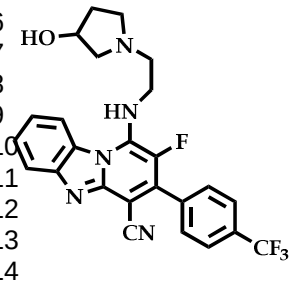

69

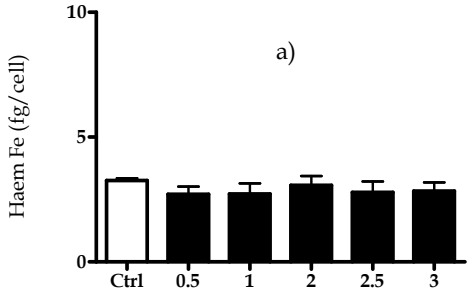

Multiples of IC_{50} for **69**

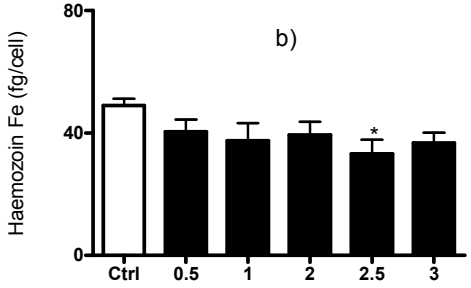

Multiples of IC_{50} for **69**

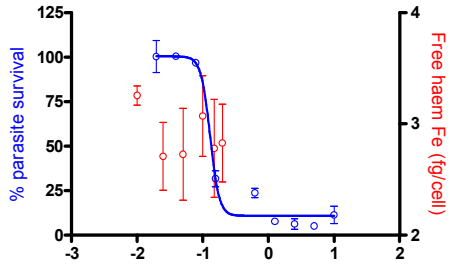

Compound **69** [log ug/ml]

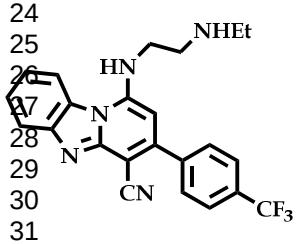

8

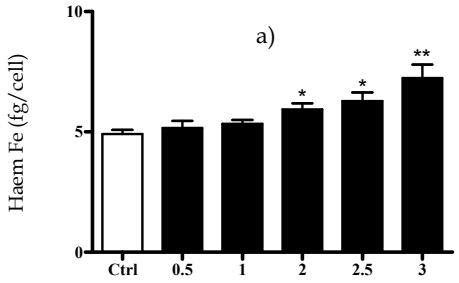

Multiples of IC_{50} for **8**

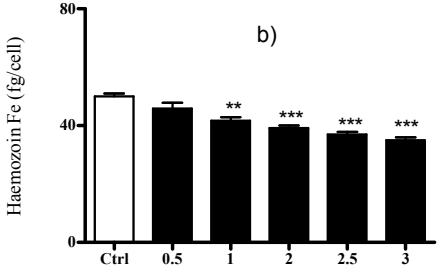

Multiples of IC_{50} for **8**

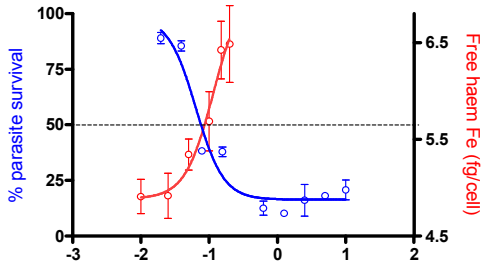

Compound **8** [log ug/ml]

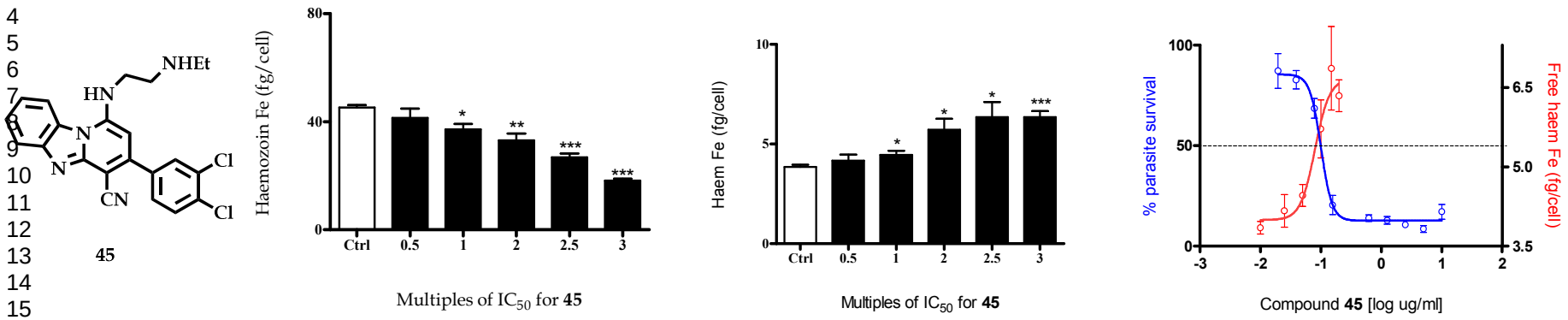

Figure 6: Haem species/fractions in synchronized drug-treated and control *Pf*NF54 parasites. Plots **a**) and **b**) respectively show free haem and haemozoin represented in terms of iron(Fe) measured in fg/cell with asterisks indicating statistical significance relative to control (*p < 0.05; ** p < 0.01 and *** p < 0.001). Parasite survival (blue) overlaid against free haem Fe (red) plots show an unambiguous trend of increasing level of free haem corresponding with parasite death only in haemozoin inhibitors in **c**)

Scheme 1: Synthesis of pyrido[1,2-*a*]benzimidazole derivatives [a]

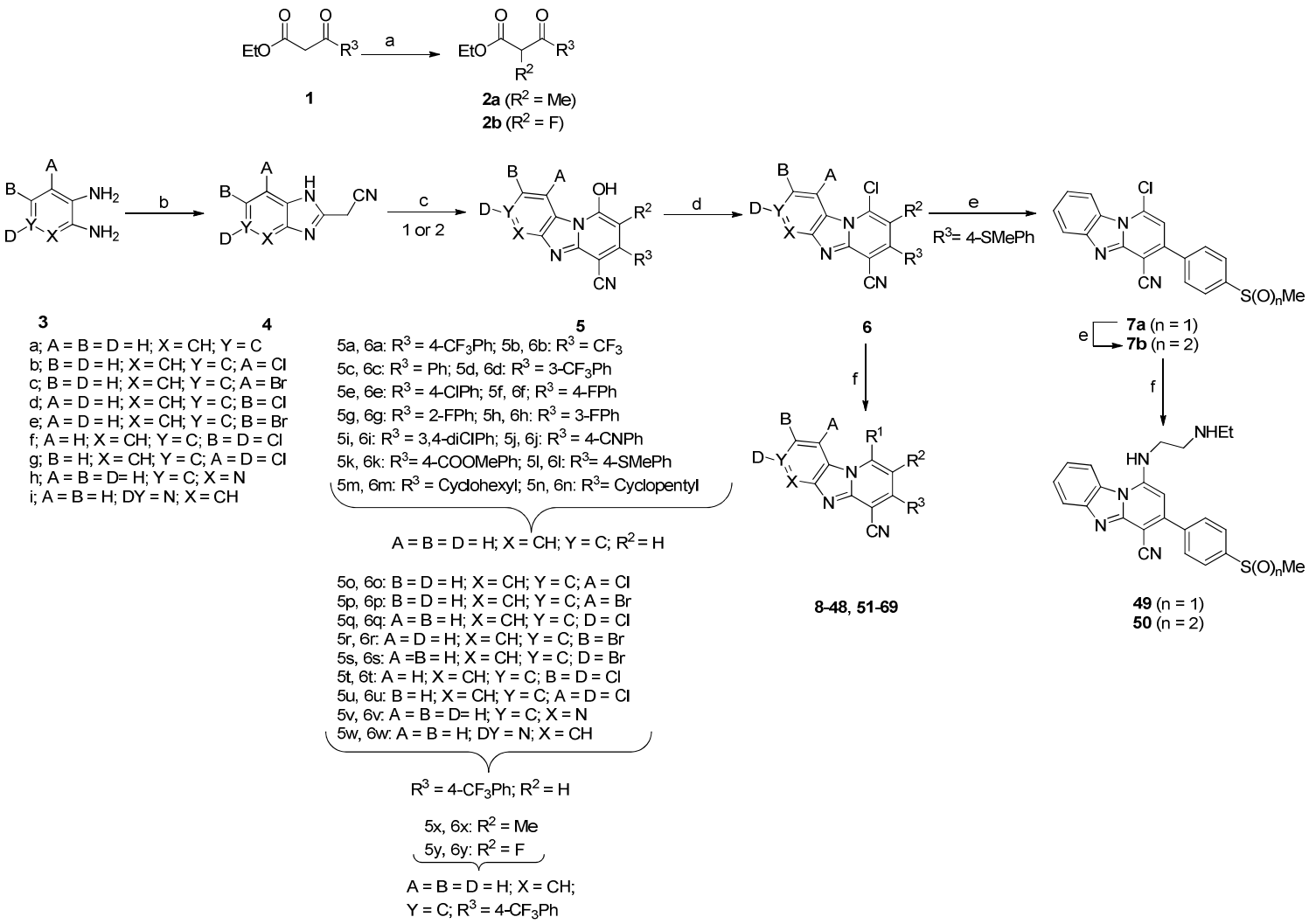

[a]Reagents and conditions: (a) For R^2 = Me: MeI, K_2CO_3, MeCN, 50 °C, 2 h (**2a**, 52%) or for R^2 = F:Selectfluor, MeCN, microwave (150 W), 82 °C, 10 min (**2b**, 66%);(b) Ethylcyanoacetate, DMF, MW, 110 °C, 15-45 min; (c) NH_4OAc, 150 °C, 1h; (d) $POCl_3$, 130 °C, 2h; (e) *m*CPBA, DCM, 0 °C, 1.5 h; (f) Amine, Et_3N, THF, 80 °C, MW, 20 min. R^1 as defined in **Tables 1, 3**.

Table 1: In vitro antiplasmodial evaluation of pyrido[1,2-*a*]benzimidazoles **8** - **38** (SAR_1)

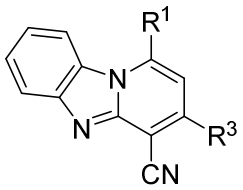

Compound	R^1	R^3	Antiplasmodial Activity [a], [b]IC_{50} (μM)		Cytotoxicity	
			*Pf*NF54	*Pf*K1	CHO IC_{50} (μM)	SI
8	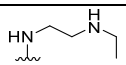	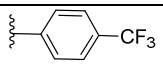	0.12	0.11	1.56	13
9	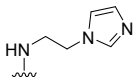	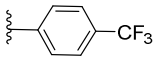	0.39	0.79	10.50	27
10	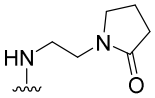	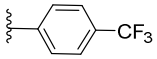	5.99			
11	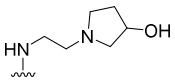	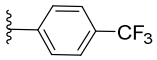	0.04	0.03	6.12	153
12	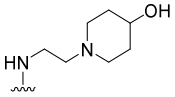	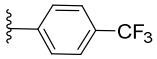	1.10			
13	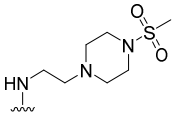	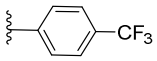	>10			
14	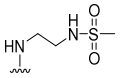	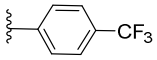	9.10			
15	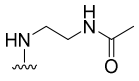	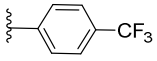	16.42			
16	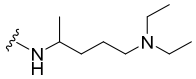		4.13			
17	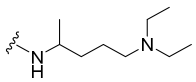	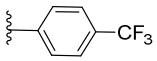	0.69	0.40	2.91	4

18	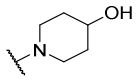	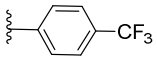	>24			
19	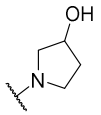	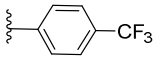	8.48			
20	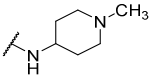	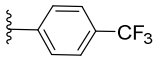	0.44	1.00	5.98	14
21	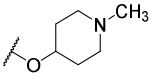	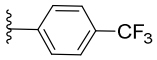	0.70	0.96	4.07	6
22	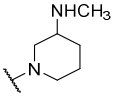	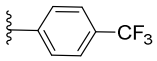	1.38			
23	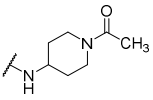	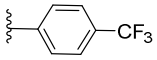	4.42			
24	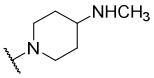	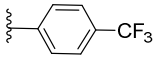	0.84	0.90	6.31	8
25	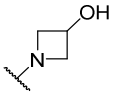	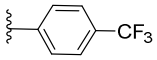	21.32			
26	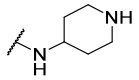	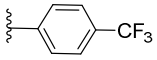	0.36	0.82	16.50	46
27	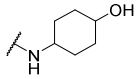	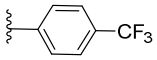	>10			
28	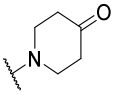	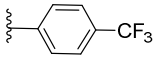	>10			
29	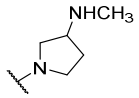	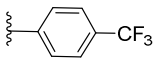	1.14			
30	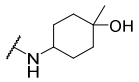	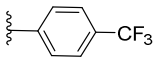	6.45			
31	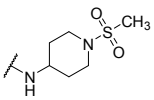	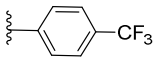	5.02			

32	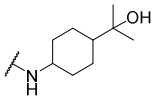	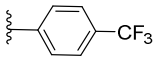	4.96			
33	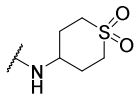	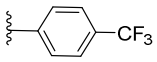	7.81			
34	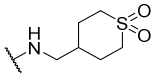	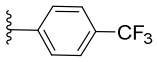	>10			
35	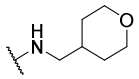	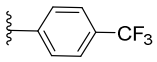	>10			
36	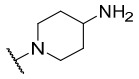	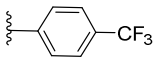	0.95	0.70	15.80	17
37	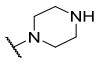	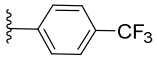	3.00	0.44		
38	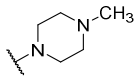	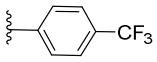	7.26	0.46		
Emetine					0.095	

[a]Mean from n values of ≥2 independent experiments with multidrug resistant (K1) and CQ-sensitive (NF54) strains of *P. falciparum*.

[b]Chloroquine (CQ) and artesunate (AS) were used as reference drugs in all experiments. Against *Pf*NF54 and *Pf*K1, our laboratory standard IC_{50} values for CQ and AS are 0.016 µM / 0.194 µM and 0.004 µM / 0.003 µM (mean from ≥10 independent assays).

CHO = Chinese Hamster Ovarian cells; SI = Selectivity Index = [IC_{50} CHO / IC_{50} NF54]

Table 2: In vitro antiplasmodial evaluation of pyrido[1,2-*a*]benzimidazoles **39** – **53** (SAR_3)**.**

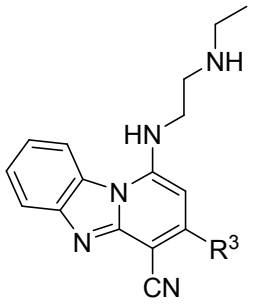

Compound	R^3	Antiplasmodial Activity [a, b] IC_{50} (µM)		Cytotoxicity	
		*Pf*NF54	*Pf*K1	CHO IC_{50} (µM)	SI
8	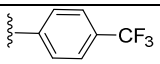	0.12	0.11	1.56	13
39		0.70	1.07	18.30	26
40	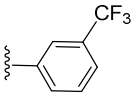	0.21	0.34	5.92	28
41	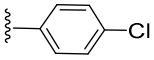	0.66	0.43	9.60	15
42	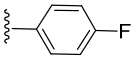	0.33	0.54	11.50	35
43		0.89	1.00	24.40	27
44	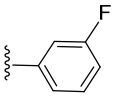	0.38	1.00	5.18	13
45	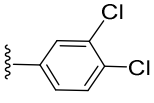	0.11	0.12	1.55	14
46	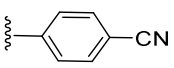	0.17	0.20	3.90	23

47	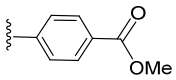	1.56			
48	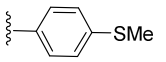	3.90			
49	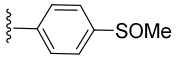	3.81			
50	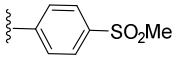	0.31	0.33	204	658
51		2.93			
52	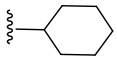	0.47	0.67	3.19	7
53		0.83	0.82	3.77	5
Emetine				0.095	

[a] Mean from n values of ≥2 independent experiments with multidrug resistant (K1) and CQ-sensitive (NF54) strains of *P. falciparum*

[b]Chloroquine (CQ) and artesunate (AS) were used as reference drugs in all experiments. Against *Pf*NF54 and *Pf*K1, our laboratory standard IC_{50} values for CQ and AS are 0.016 μM / 0.194 μM and 0.004 μM / 0.003 μM (mean from ≥10 independent assays).

CHO = Chinese Hamster Ovarian cells; SI = Selectivity Index = [IC_{50} CHO / IC_{50} NF54]

Table 3: In vitro antiplasmodial evaluation of pyrido[1,2-*a*]benzimidazoles **54 – 69** (SAR_2).

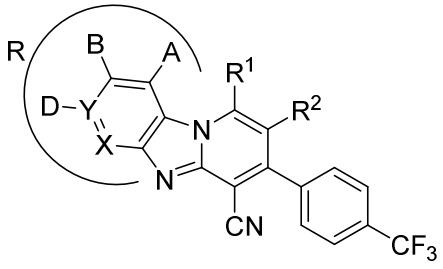

Compound	R	R^1	R^2	Antiplasmodial Activity [a, b] IC_{50} (µM)		Cytotoxicity	
				*Pf*NF54	*Pf*K1	CHO IC_{50} (µM)	SI
8		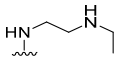	H	0.12	0.11	1.56	13
54	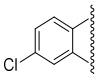	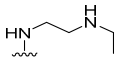	H	0.03	0.03	8.71	362
55	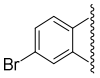	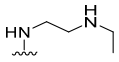	H	0.38		1.80	5
56	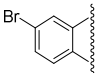	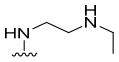	H	0.07		4.44	63
57		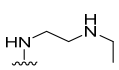	H	0.14	0.26	1.63	5
58		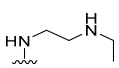	H	0.15	0.24	1.55	2
59	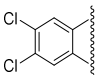	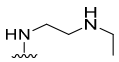	H	0.02	0.02	3.39	188
60	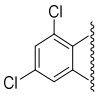	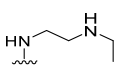	H	0.03	0.04	11.20	431
61	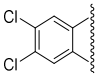	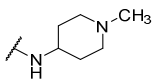	H	0.05	0.19	4.19	6.1

62	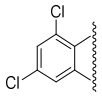	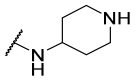	H	0.26		5.90	22.3
63	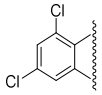	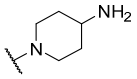	H	0.18	0.21	2.98	7.3
64		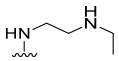	H	0.14	0.13	4.10	5
65		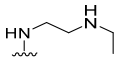	H	0.27	0.84	3.14	6
66		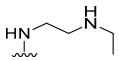	Me	1.28			
67		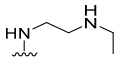	F	5.53			
68		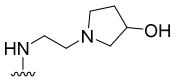	Me	0.55	0.47	25.0	45
69		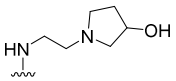	F	0.19	0.17	206	1084
Emetine						0.095	

[a] Mean from n values of ≥2 independent experiments with multidrug resistant (K1) and CQ-sensitive (NF54) strains of *P. falciparum*

[b]Chloroquine (CQ) and artesunate (AS) were used as reference drugs in all experiments. Against *Pf*NF54 and *Pf*K1, our laboratory standard IC_{50} values for CQ and AS are 0.016 µM / 0.194 µM and 0.004 µM / 0.003 µM (mean from ≥10 independent assays).

CHO = Chinese Hamster Ovarian cells; SI = Selectivity Index = [IC_{50} CHO / IC_{50} NF54]

Table 4: Physicochemical properties and in vitro microsomal stability of selected pyrido[1,2-*a*]benzimidazoles

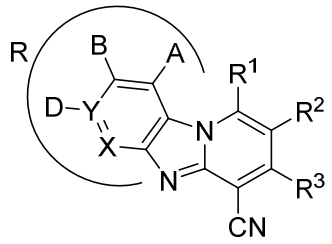

Compound	R	R^1	R^2	R^3	LogP [b]	Melting Point (°C)	Kinetic Solubility (μM)	Permeability (log P_{app}, class) [c]		Met Stability (% remaining after 30mins)	
							pH6.5	pH4.0	pH6.5	MLMs	HLMs
8		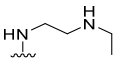	H	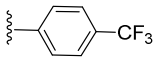	4.7	222–224	<5	-6.9, low	-4.3, high	97	84
11		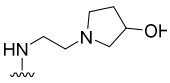	H	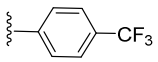	4.0	267–269	<5	-7.2, low	-4.9, high	51	
12		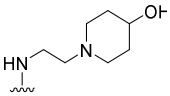	H	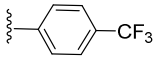	4.1	310–312	<5				
17		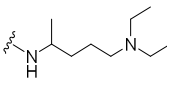	H	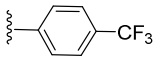	6.2	220–222	85	-6.4, mod	-3.5, high	32	53
20		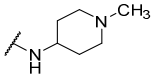	H	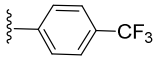	4.6	215–217	<5	-7.0, low	-3.8, high	63	75
26		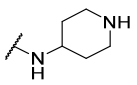	H	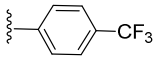	4.3	>270				65	99
36		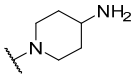	H	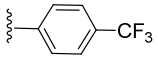	4.5	233–235	<5		-5.7, mod	92	91
44		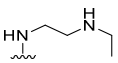	H	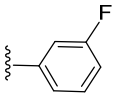	3.9	203–205	25	-7.1, low	-5.0, high	100	89
45		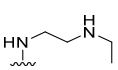	H	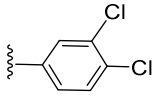	4.8	235–237				65	60

50		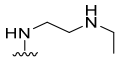	H	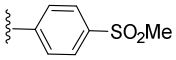	2.4	227–230	40	-6.4, mod	-6.7, low	86	
52		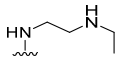	H	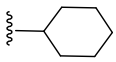	4.0	216–218	10			42	
54		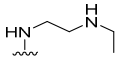	H	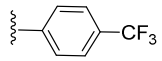	5.2	224–227				75	87
57		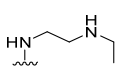	H	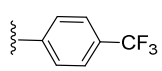	5.2	223–225	10	-7.2, low	-4.0, high	93	89
59		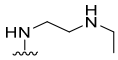	H	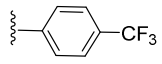	5.8	305–307	10		-6.5, mod	81	95
60		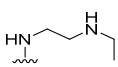	H	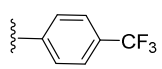	5.8	319–321	20		-4.9, high	87	87
64		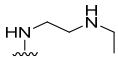	H	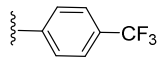	4.5	225–227	10		-4.2, high		
66		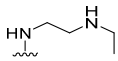	Me	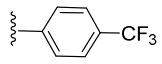	5.1	236–238	<5		-5.4, mod	80	85
67		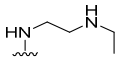	F	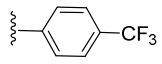	4.8	293–295	160		-5.2, high	35	39
68		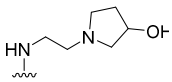	Me	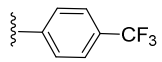	4.5	236–238	<5		-3.9, high		
69		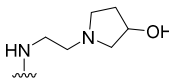	F	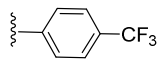	4.2	265–267	80		-5.3, high	37	
Warfarin								-3.7, high	-3.8, high		
Propanolol								-5.9, low	-4.4, high		
Testosterone								-3.8, high	-3.7, high		
Midazolam										1.3	0.1
MMV390048[a]										94	93

[a] Reference [26]

[a] (3-[2-(Trifluoromethyl)pyridin-5-yl]-5-[4-(methylsulfonyl)-phenyl]pyridin-2-amine

[b] Predicted from ChemBioDraw Ultra version 14.0

[c] Low permeability log Papp<-6.5; moderate permeability (mod) log Papp -6.5 to -5.5; high permeability log Papp>-5.5

Table 5: In vivo oral efficacy of selected pyrido[1,2-*a*]benzimidazoles in *P. berghei*-infected Mice.

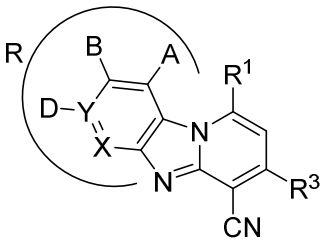

Code	R	R^1	R^3	*Pf*NF54 IC_{50} (μM)	Oral Dose [a] (mg/kg)	% Reduction in parasitemia (MSD) [b]	Cured/ Infected
8		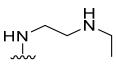	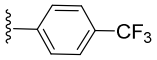	0.12	4 x 50 4 x 25 4 x 12.5 4 x 6 4 x 3	96.0 (14)[c] 96.0 (14)[c] 81.0 (14)[c] 38.0 (7)[c] 0 (4)[c,d]	0/3 0/3 0/3 0/3 0/3
44		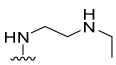	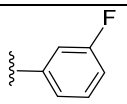	0.38	4 x 50	61.0 (24)	1/3
57		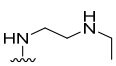	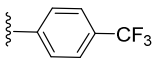	0.14	4 x 50	85.0 (7)	0/3
59	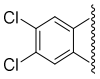	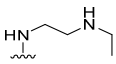	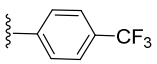	0.02	4 x 50 4 x 30 4 x 10 4 x 3	98.0 (30) 99.7 (30) 99.6 (18) 99.5 (17)	3/3 3/3 0/3 0/3
60	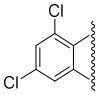	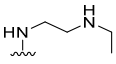	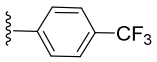	0.03	4 x 50 4 x 30 4 x 10 4 x 3	98.0 (30) 99.4 (30) 99.4 (18) 99.4 (16)	3/3 2/3 0/3 0/3

Chloroquine [e]	0.016	4 x 30	99.9 (24)	0/10
Control		-	- (4) [d]	

[a]Test compounds were formulated in 90/10 Tween80/ethanol (v/v), diluted 10 times with water and administered orally once per day on 4 consecutive days (4, 24, 48, and 72 h after infection).

[b]MSD = mean survival time in days.

[c]Used the HCl salt.[11]

[d]Mice with < 40 % parasitemia reduction were euthanized on day 4 in order to prevent death otherwise occurring at day 6.

[e]Data from Le Manach et al.,2014.[27]

Table 6: Pharmacokinetic parameters for **59** and **60** in mice

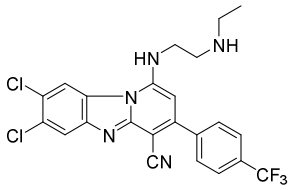

59

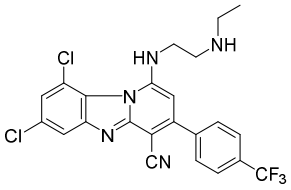

60

Parameter	**i.v. (2.5mg/kg)** [a]	**p.o. (10mg/kg)** [b]	**i.v. (2.5mg/kg)** [a]	**p.o. (10mg/kg)** [b]
$t_{1/2}$ (h) [c]	15	15	21	21
C_{max} (µM)	-	0.07	-	0.22
T_{max} (h)	-	10	-	>10
V_d (L/kg) [c]	26	-	19	-
CL (mL/min/kg) [c]	21	-	11	-
$AUC_{0-\infty}$ (µM/L.min) [c]	256	158	571	686
Oral bioavailability (%) [c]	-	<15	-	30

[a]For intravenous dosing(n=3 mice), compounds were formulated in a solution of dimethylacetamide, polyethylene glycol and propylene glycol/ethanol mixture 4:1 at a ratio 1:3:6.[b] For oral dosing (n=3 mice), compounds were formulated as suspension in 100% HPMC.

[c] PK exposure parameters derived from the population parameters of the pharmacometric model

Table 7: In vitro activity against *Pf*NF54 gametocytes and *P. berghei* liver stage

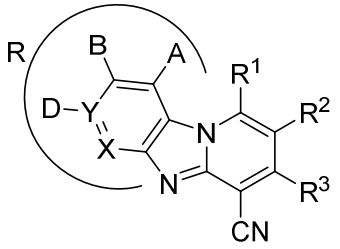

Compound	R	R[1]	R[2]	R[3]	LG gametocyte IC_{50} (μM) [a]	Fold Change [d] (stage preference EG^c/LG)	*P. berghei* Liver IC_{50} (μM)	*Pf*NF54 IC_{50} (μM)
8		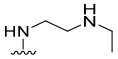	H	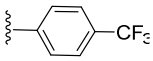	0.62[b]	2.4 (LG)		0.12
9		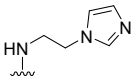	H	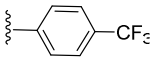	1.02	1.1 (LG)		0.39
17		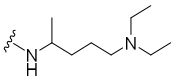	H	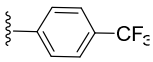	3.02	0.7 (EG)		0.69
26		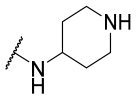	H	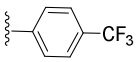	1.16	1.6 (LG)	3.31	0.36
39		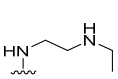	H		1.44	-		0.70
40		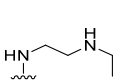	H	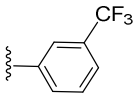	0.49	1.6 (LG)		0.21
41		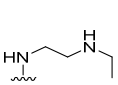	H	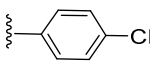	0.69	1.5 (LG)		0.66
42		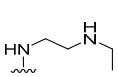	H	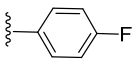	1.77	2.1 (LG)		0.33
44		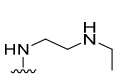	H	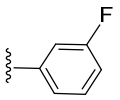	3.63	1.2 (LG)		0.38
45		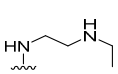	H	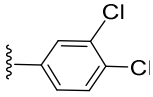	0.59	1.2 (LG)		0.11

46	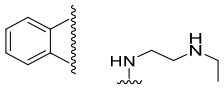		H	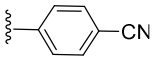	2.66	1.3 (LG)		0.17
47	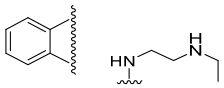		H	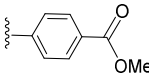	1.68	1.4 (LG)		1.56
52	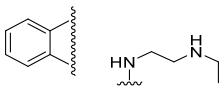		H	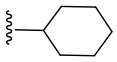	0.46	3.3 (LG)		0.47
53	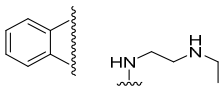		H		0.67	1.7 (LG)		0.83
54	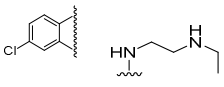		H	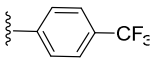	0.82 [b]	1.1 (LG)		0.03
59	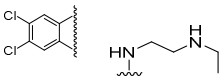		H	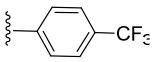	0.72	1.2 (LG)		0.02
60	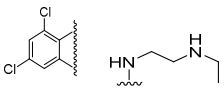		H	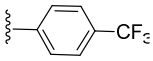	1.44 [b]	1.2 (LG)		0.03
66	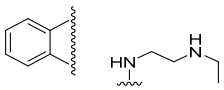		Me	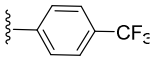	2.57	0.8 (EG)	2.85	1.28
69	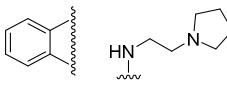		F	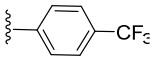	-	-	1.42	0.19
MB					0.14			
PMQ							8.42	
ATQ							0.001 [e]	

[a] LG (late stage IV/V gametocytes) data were generated using the ATP assay.

[b] Data generated using the luciferase reporter assay.

[c] EG = Early gametocytes (stage II/III); LG (late stage IV/V gametocytes), data generated in parallel assays with the luciferase reporter assay, stage preference = EG/LG IC_{50}

[e] Data adopted from Ref 16.

MB = Methylene blue; PMQ = Primaquine; ATQ = Atovaquone

TABLE OF CONTENT GRAPHIC:

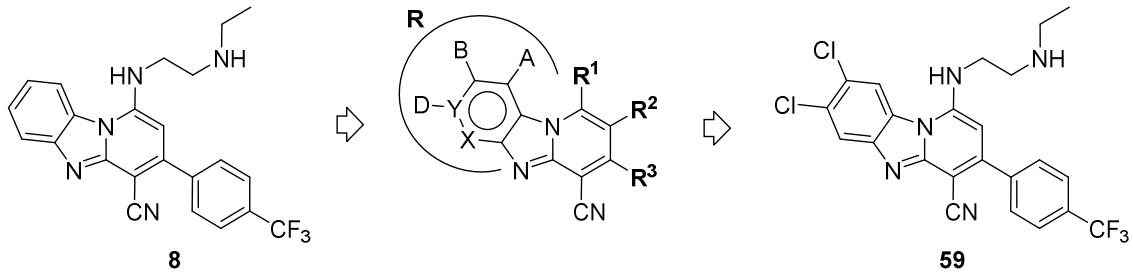

8

IC_{50} *Pf*NF54 = 120 nM; *Pf*K1 = 110 nM
in vivo *P. berghei* (HCl salt: p.o.) 4×25 mg/kg = 95.7%
0/3 malaria infected mice cured

59

IC_{50} *Pf*NF54 = 18 nM; *Pf*K1 = 19nM
in vivo *P. berghei* (p.o.) 4×30 mg/kg = 99.7%
3/3 malaria infected mice cured

Keywords: antiplasmodial activity, pyrido[1,2-*a*]benzimidazoles, in vivo efficacy, structure activity relationship, haemozoin inhibition, antimalarial, *Plasmodium falciparum*, microsomal stability